

Immersion Freezing of Coal Combustion Ash Particles from the Texas Panhandle

Craig Whiteside¹, Yutaka Tobo², Sarah Brooks³, Oliver Mulamba¹, Jessica Mirrielees³, and Naruki Hiranuma⁴

¹West Texas A & M University

²National Institute of Polar Research

³Texas A&M University

⁴West Texas A&M University

November 24, 2022

Abstract

Coal combustion aerosol particles contribute to the concentrations of ice-nucleating particles (INPs) in the atmosphere. Especially, immersion freezing can be considered as one of the most important mechanisms for INP formation in supercooled tropospheric clouds that exist at temperatures between 0°C and -38°C. The U.S. contains more than 550 operating coal-burning plants consuming 7.2×10^8 metric tons of coal (in 2016) to generate a total annual electricity of >2 billion MW-h, resulting in the emission of at least 4.9×10^5 metric tons of PM10 (particulate matter smaller than 10 μm in diameter). In Texas alone, 19 combustion plants generate 0.15 billion MW-h electricity and $>2.4 \times 10^4$ metric tons of PM10. Here we present the immersion freezing behavior of combustion fly ash and bottom ash particles collected in the Texas Panhandle region. Two types of particulate samples, namely <45 μm sieved bottom ash (B_Ash_TX_PH) and <45 μm sieved fly ash (F_Ash_TX_PH), were prepared. Afterwards, their immersion freezing abilities were measured using the Cryogenic Refrigerator Applied to Freezing Test (CRAFT) system covering the heterogeneous freezing temperature down to -30 °C. The results were generated and are reported through two metrics, frozen fraction, $f_{\text{frozen}}(T)$, and ice nucleation active site density per unit mass, $\text{nm}(T)$ as a function of temperature. Our preliminary results show that an onset increase in $f_{\text{frozen}}(T)$ for B_Ash_TX_PH (f_{frozen}) occurred as high as at -15°C, whereas the onset for F_Ash_TX_PH is at -18°C. Secondly, B_Ash_TX_PH exhibited a higher $\text{nm}(-20 \text{ }^\circ\text{C})$ of 10^5 g^{-1} than that of F_Ash_TX_PH ($5 \times 10^3 \text{ g}^{-1}$). On the other hand, previous studies on different combustion ash samples have reported that the opposite trend (i.e., ice nucleation efficiency of fly ash is greater than that of bottom ash; Grawe et al., 2016, ACP; Umo et al., 2015, ACP). We will discuss possible reasons for the observed differences. In addition, the results of complementary physico-chemical analyses via X-ray diffraction technique, Raman microscopy and scanning electron microscopy on both ash types will also be presented to relate the crystallographic and chemical properties to their ice nucleation abilities.

Overview

Immersion freezing is a primary pathway for the development of ice nucleating particles (INPs) in super-cooled water droplets in the atmosphere, which can impact local weather and public health (i.e. hail formation and air quality). The diversity and quantity of INPs has influenced investigation into the physico-chemical properties of coal combustion ash. We examined the molecular composition, nanoscale surface morphology, and freezing efficiency for two by-products of coal combustion relevant to the local Texas Panhandle region, specifically fly ash (F_Ash_TX_PH) and bottom ash (B_Ash_TX_PH) (sieved to <45µm). We demonstrate the diversity between the coal combustion ash by-products and their effect on ice nucleation efficiency.

Coal Combustion Ash in Texas Panhandle

In Texas, 19 reporting coal burning facilities produce >24,000 metric tons of PM₁₀, for Potter County, TX in 2014, nearly 900 metric tons of PM₁₀ (course particles) and PM_{2.5} (fine particles) were emitted into the atmosphere from coal combustion. We analyzed coal combustion fly ash and bottom ash samples, a heterogeneous mixture of inorganic and organic compounds, representative to the Texas Panhandle using various techniques. F_Ash_TX_PH and B_Ash_TX_PH are similar in composition consisting mainly of aluminum oxide (Al₂O₃), quartz (SiO₂), calcium oxide (CaO), and magnesium oxide (MgO), which can vary based on type of coal (anthracite, bituminous/sub-bituminous, lignite) and the combustion process.

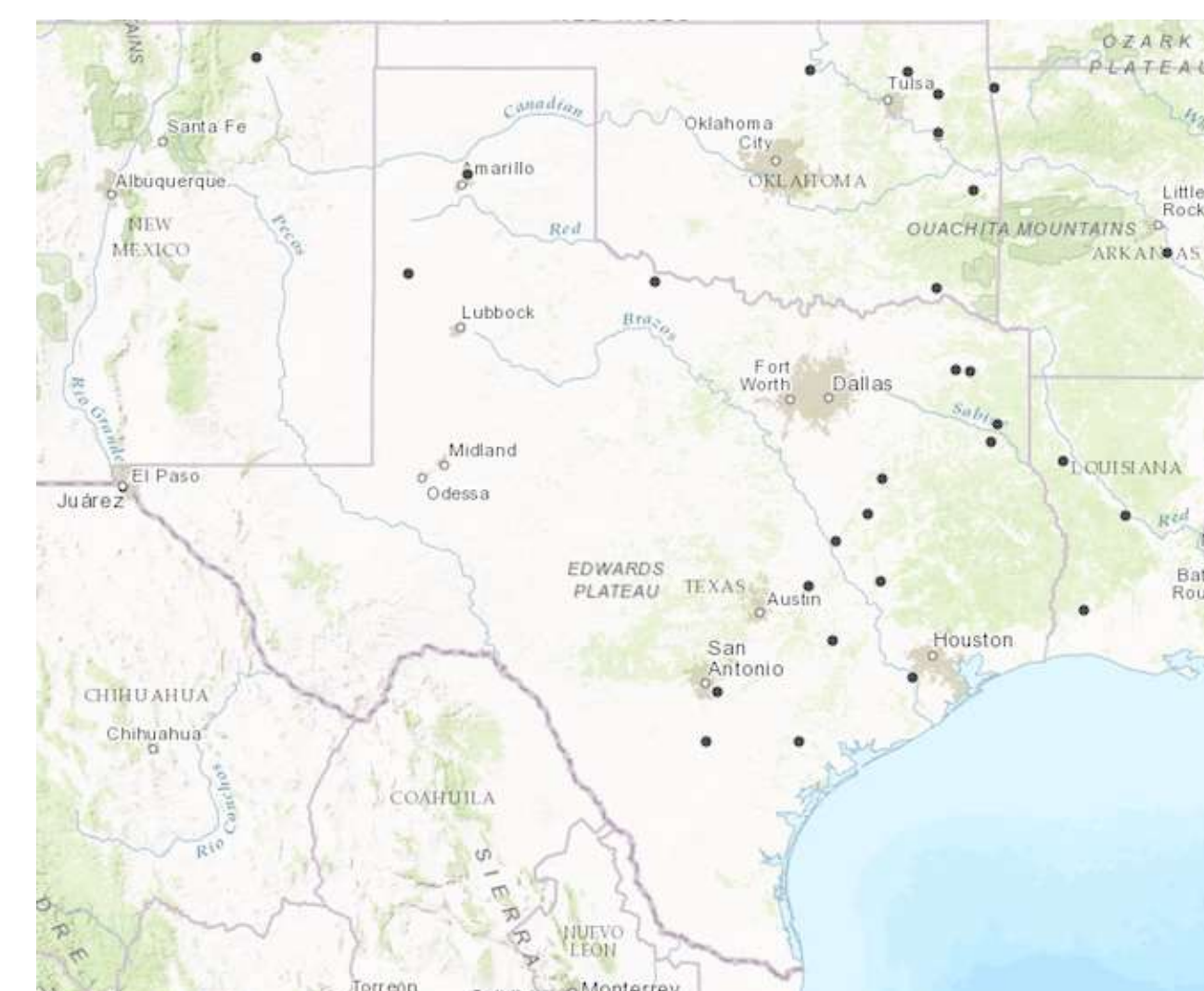


Fig. 1. Locations of coal combustion plants in Texas (2014)

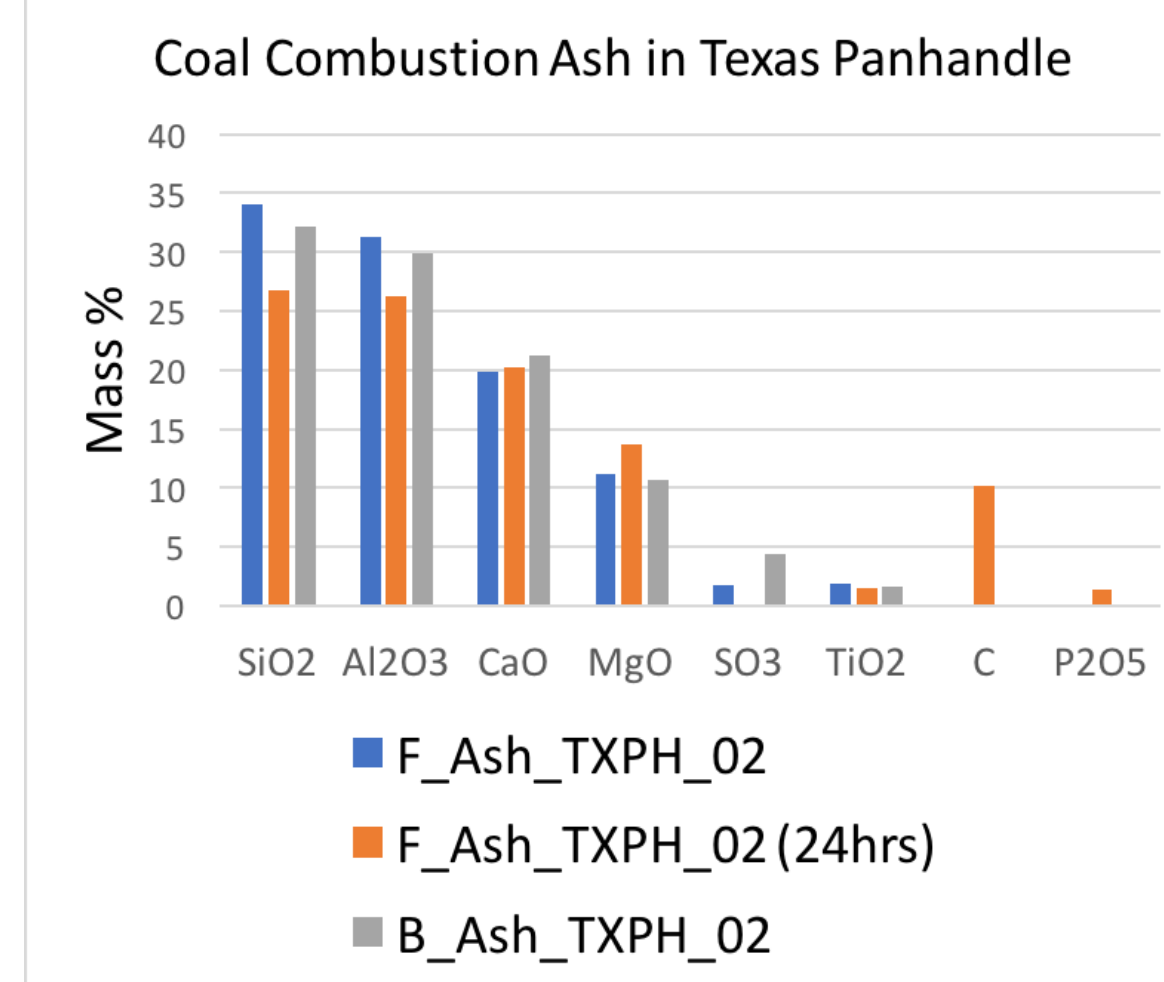


Fig. 2. SEM-EDS mass(%) of oxides contained in bottom and fly ash samples

Method

Preserved coal fly ash and bottom ash samples were first dried at room temperature ~20°C for 48 hours. Secondly, the ash samples were sieved to ≤ 45µm diameters in a 3-stage cascade of New Perlon Sieves (≤ 1000µm → ≤ 180µm → ≤ 45µm) using a Retsch AS200 Sieve Shaker. These samples were used for the further investigation namely F_Ash_TX_PH_02 and B_Ash_TX_PH_02. Suspension were prepared in a known volume of Milli-Q purified water (18.2 MΩ cm resistivity, TOC < 4ppb) using a known mass to create a 1 mg/mL mass concentration (0.1wt%) then diluted tenfold based on each specific experiment.

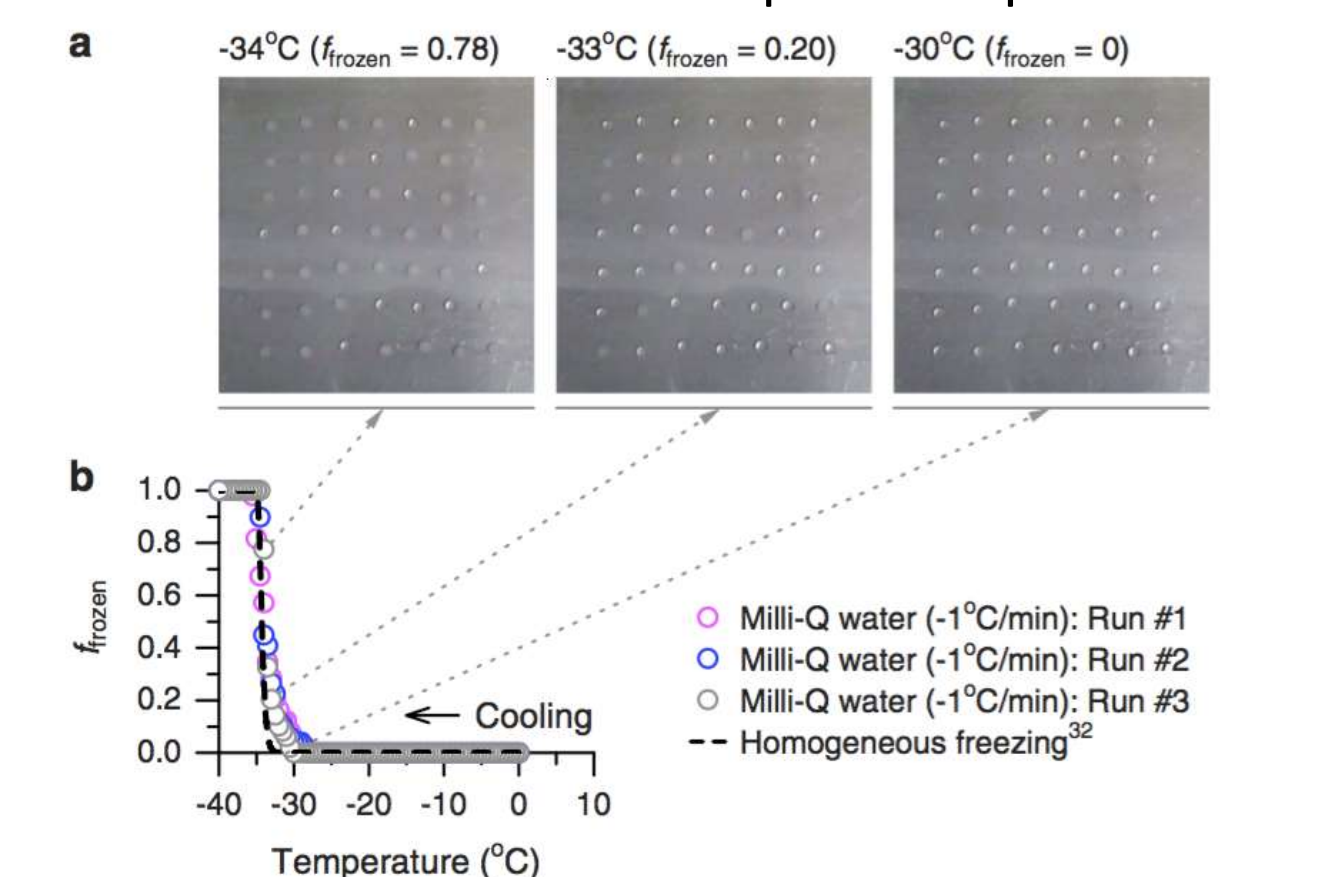


Fig. 3. Fraction of frozen droplets as a function of temperature carried out by Tobo (2016) using the CRAFT system (a) images captured by convention WEB camera (b) fraction of frozen droplets (f_{frozen}) of ultrapure water

Ice Nucleation Experiment

Immersion freezing experiments using super-microliter-sized droplets (5µL) were performed in a clean booth on a AI cold-stage using the Cryogenic Refrigerator Applied to Freezing Test system (CRAFT) (Tobo, 2016) at a cooling rate of 1°C/min. The CRAFT system is located at the National Institute of Polar Research (NiPR) in Tachikawa, Japan. Visual analysis for ice nucleated droplets was determined for every 0.5°C based on transparency of droplets.

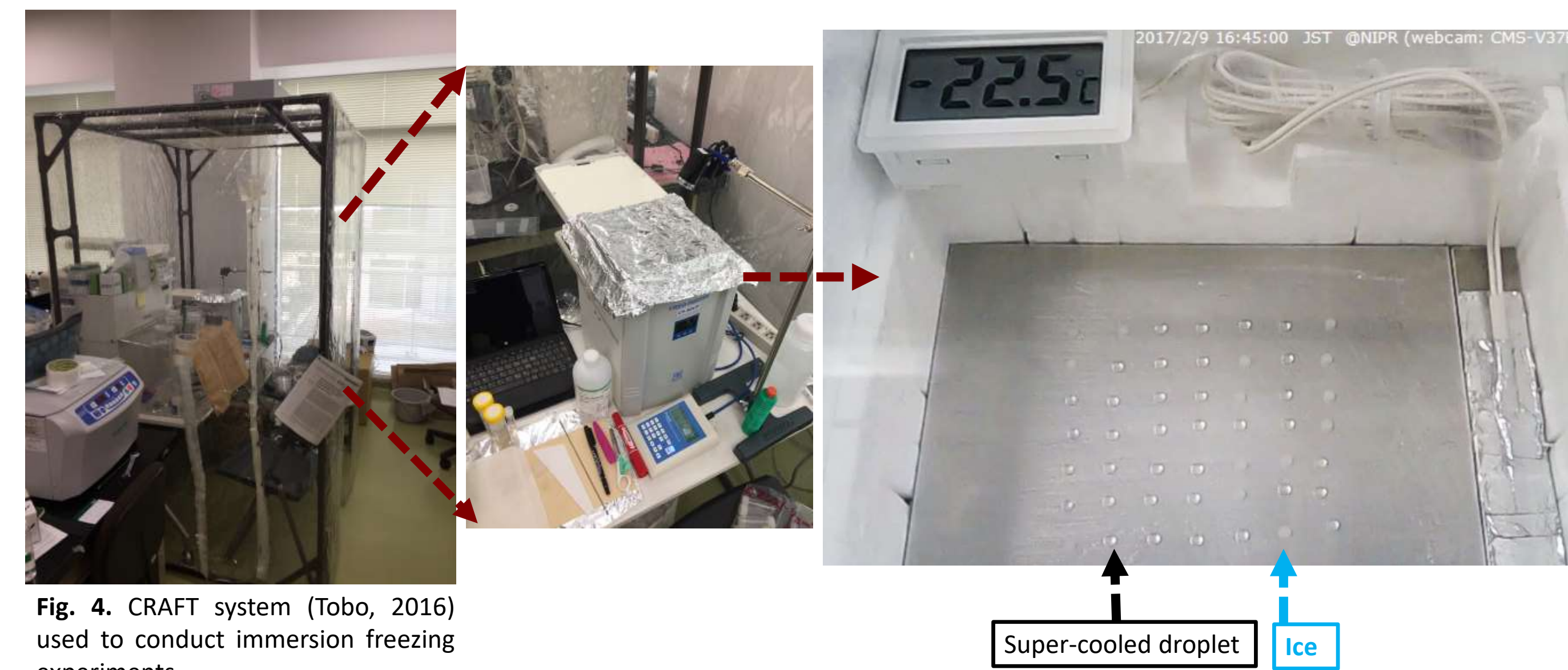


Fig. 4. CRAFT system (Tobo, 2016) used to conduct immersion freezing experiments

Ice Nucleating Ability

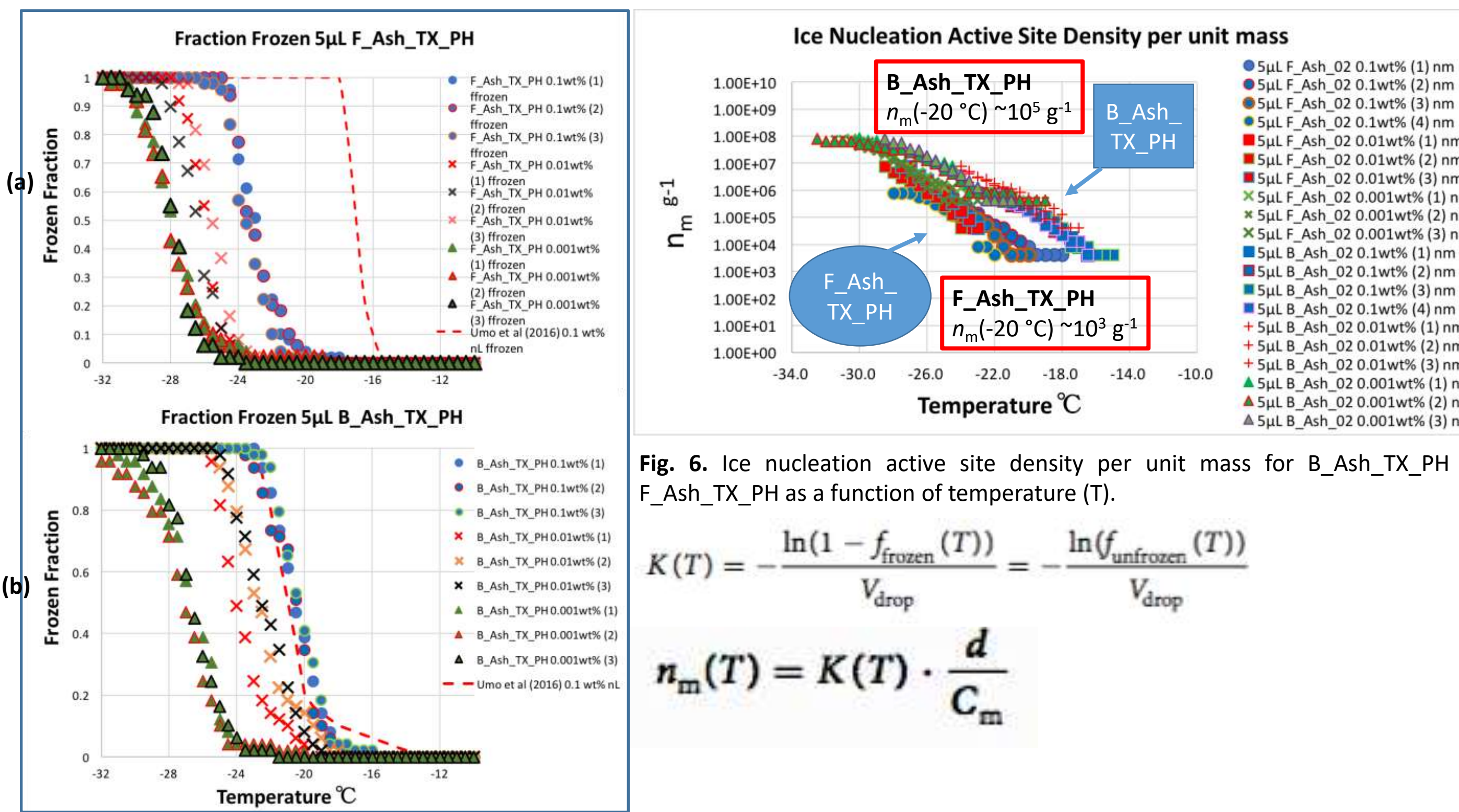


Fig. 6. Ice nucleation active site density per unit mass for B_Ash_TX_PH and F_Ash_TX_PH as a function of temperature (T).

$$K(T) = \frac{\ln(1 - f_{\text{frozen}}(T))}{V_{\text{droplet}}} = \frac{\ln(f_{\text{unfrozen}}(T))}{V_{\text{droplet}}}$$

$$n_m(T) = K(T) \cdot \frac{d}{C_m}$$

Fig. 5. Fraction of frozen droplets as a function of temperature (a) F_Ash_TX_PH

Ice Nucleation (Time Trials)

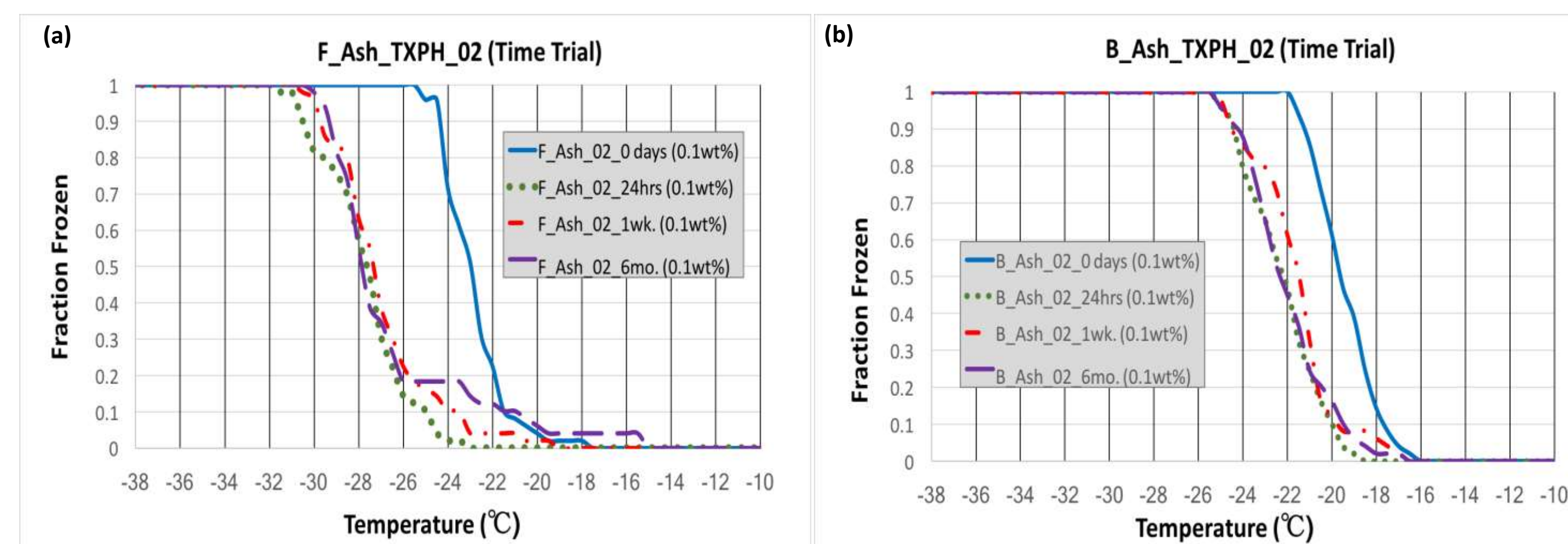
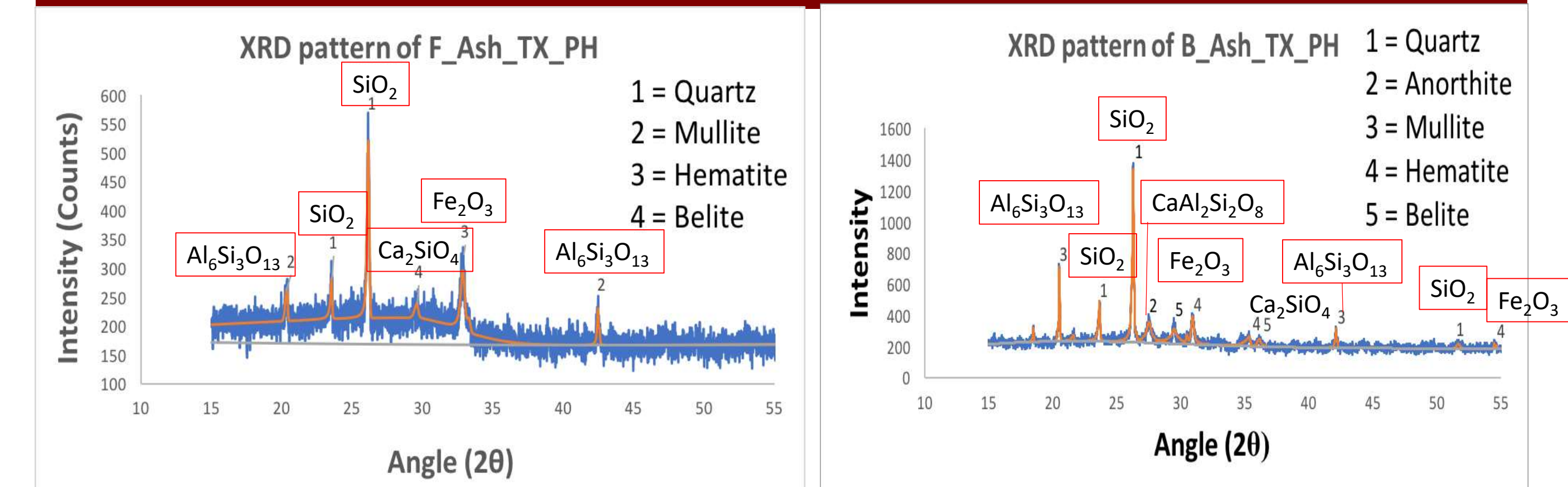


Fig. 7(a). Fraction of 3µL droplets frozen as a function of temperature of fly ash from the Texas Panhandle at a mass concentration of 1 mg/mL ~ 0.1wt% over a period of 0 days, 1 day, 1 week, and 6 months. (b) Also shown is fraction of 3µL droplets frozen as a function of temperature of bottom ash from the Texas Panhandle.

X-Ray Diffraction (XRD)



XRD patterns indicate mineralogy phases and intensity for F_Ash_TX_PH and B_Ash_TX_PH. A key difference is the presence of anorthite (CaAl₂Si₂O₈) in B_Ash_TX_PH

Surface Morphology

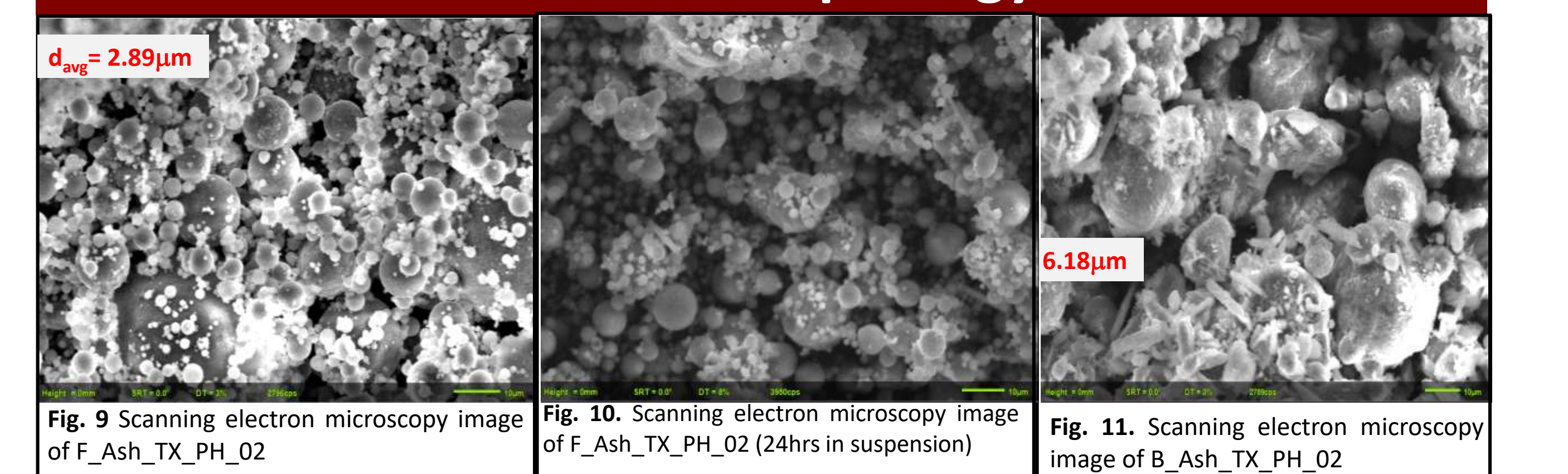


Fig. 9. Scanning electron microscopy image of F_Ash_TX_PH_02

Fig. 10. Scanning electron microscopy image of F_Ash_TX_PH_02 (24hrs in suspension)

Fig. 11. Scanning electron microscopy image of B_Ash_TX_PH_02

Raman Spectroscopy

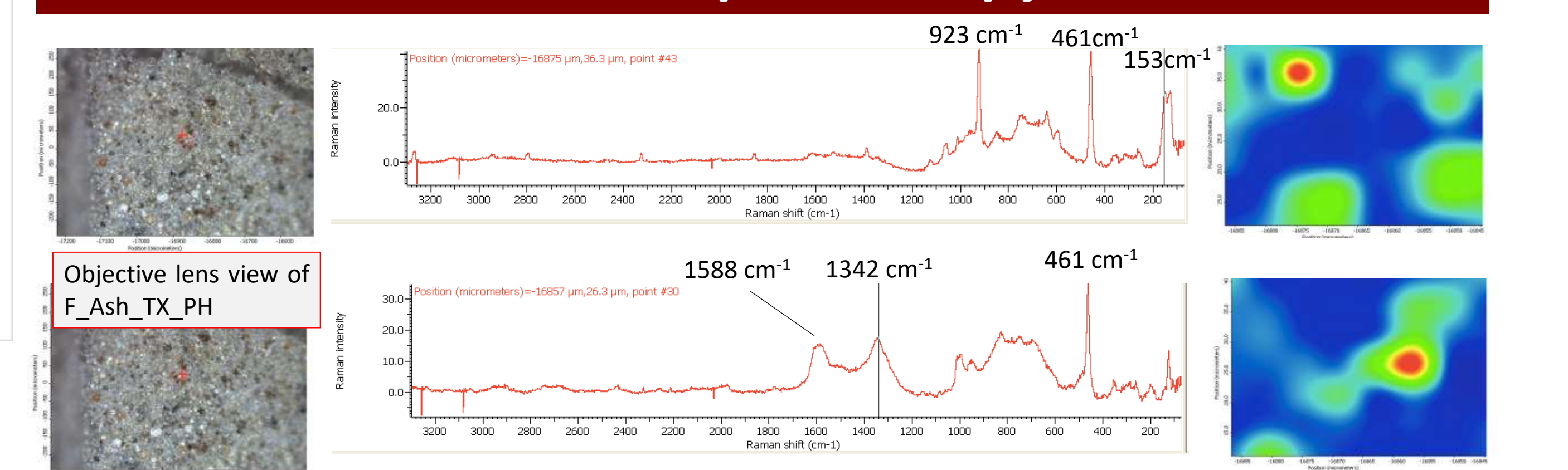


Fig. 11. Raman spectra of F_Ash_TX_PH excited at 532 nm with 5mW power measured between frequencies (3300cm⁻¹ -100cm⁻¹). The 56 points were analyzed in an area with a step size of X=6 µm by Y=5 µm.

Classification of combustion ash from the Texas Panhandle	Sample Name	B_Ash_01 (Bulk)	B_Ash_02 (<45µm)	F_Ash_01 (Bulk)	F_Ash_02 (<45µm)	F_Ash_02 (24hr)
Number of Spectra Recorded		25	12	28	66	20
Disordered Graphite (%)		32	67	46	44	80
Disordered Graphite + Organic (%)		0	8	0	0	0
Disordered Graphite + Inorganic (%)		4	33	18	11	35
Disordered Graphite + Organic + Inorganic (%)		28	17	29	33	45
Only Organic (%)		0	17	4	2	0
Only Inorganic (%)		12.5	33	57	33	15
Inorganic + Organics Internal mixtures (%)		87.5	50	39	65	85
Total (%)		100	100	100	100	100

Summary & Outlook

Summary

- Coal combustion ash consist mainly of insoluble inorganic minerals
- Differences in surface morphologies of coal fly ash and bottom ash
- B_Ash_TX_PH is a more efficient INP as compared to F_Ash_TX_PH

Next Steps

- Elemental analysis using SEM-EDX
- Dispersion modelling (HYSPPLIT)

Acknowledgements

Craig Whiteside thanks Killgore Graduate Research Grant for the funding support. Whiteside and Y. Tobo want to thank the National Institute of Polar Research for the travel fellowship support. C. Whiteside acknowledges Dr. William J. Rogers for providing ash samples. N. Hiranuma acknowledges partial financial support by the Higher Education Assistance Fund (HEAF).